SIMPEL: Circuit model for photonic spike processing laser neurons

Bhavin J. Shastri , Mitchell A. Nahmias, Alexander N. Tait, Ben Wu, and Paul R. Prucnal

Department of Electrical Engineering, Princeton University, Princeton NJ, 08544, USA

shastri@ieee.org

Abstract: We propose an equivalent circuit model for photonic spike processing laser neurons with an embedded saturable absorber—a simulation model for photonic excitable lasers (SIMPEL). We show that by mapping the laser neuron rate equations into a circuit model, SPICE analysis can be used as an efficient and accurate engine for numerical calculations, capable of generalization to a variety of different types of laser neurons with saturable absorber found in literature. The development of this model parallels the Hodgkin–Huxley model of neuron biophysics, a circuit framework which brought efficiency, modularity, and generalizability to the study of neural dynamics. We employ the model to study various signal-processing effects such as excitability with excitatory and inhibitory pulses, binary all-or-nothing response, and bistable dynamics.

References and links

1. F. Selmi, R. Braive, G. Beaudoin, I. Sagnes, R. Kuszelewicz, and S. Barbay, "Relative refractory period in an excitable semiconductor laser," Phys. Rev. Lett. **112**, 183902 (2014).
2. D. Brunner, M. C. Soriano, C. R. Mirasso, and I. Fischer, "Parallel photonic information processing at gigabyte per second data rates using transient states," Nat. Commun. **4,** 1364 (2013).
3. D. Woods and T. J. Naughton, "Optical computing: Photonic neural networks," Nature Phys. **8**, 257–259 (2012).
4. R. Martinenghi, S. Rybalko, M. Jacquot, Y. K. Chembo, and L. Larger, "Photonic nonlinear transient computing with multiple-delay wavelength dynamics," Phys. Rev. Lett. **108**, 244101 (2012).
5. A. Hurtado, K. Schires, I. D. Henning, and M. J. Adams, "Investigation of vertical cavity surface emitting laser dynamics for neuromorphic photonic systems," Appl. Phys. Lett. **1000**, 103703 (2012).
6. L. Appeltant, M. C. Soriano, G. V. der Sande, J. Danckaert, S. Massar, J. Dambre, B. Schrauwen, C. R. Mirasso, and I. Fischer, "Information processing using a single

13. H. Jaeger and H. Haas, "Harnessing nonlinearity: Predicting chaotic systems and saving energy in wireless communication," Science **304**, 78–80 (2004).
14. J. Hasler and H. B. Marr, "Finding a roadmap to achieve large neuromorphic hardware systems," Front. Neurosci. **7**, 118 (2013).
15. M. Mahowald and R. Douglas, "A silicon neuron," Nature **354**, 515–518 (1991).

43. D. J. Channin, "Effect of gain saturation on injection laser switching," J. Appl. Phys. **50**, 3858–3860 (1979).
44. H. Park, A. W. Fang, R. Jones, O. Cohen, O. Raday, M. N. Sysak, M. J. Paniccia, and J. E. Bowers, "A hybrid AlGaInAs-silicon evanescent waveguide photodetector," Opt. Express **15**,, 6044–6052 (2007).
45. R. S. Tucker and D. J. Pope, "Circuit modeling of the effect of diffusion on damping in a narrow-stripe semiconductor laser," IEEE J. Quantum Electron. **19**, 1179–1183 (1983).
46. P. V. Mena, S.-M. Kang, and T. A. DeTemple, "Rate-equation based laser model with a single solution regime," J. Lightw. Technol.

the dynamics of individual units, which are fundamentally driven by differential equation models.

1.1. Our contribution

Here, we propose *SIMPEL*—SImulation Model for Photonic Excitable Lasers—which bridges the gap between the underlying physics and relevant dynamics of excitable lasers by transforming its rate equations to an equivalent circuit representation. We show that this circuit
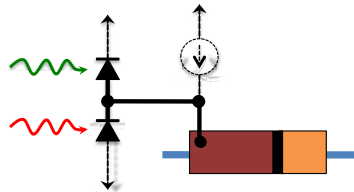
Laser Model

Fig. 1. Schematic of a biological neuron and a two-section excitable laser that share key dynamical properties. In the LIF neuron model, weighted and delayed input signals are spatially summed at the dendritic tree into an input current, which travel to the soma and perturb the internal state variable, the voltage. The soma performs integration and then applies a threshold to make a spike or no-spike decision. After a spike is released, the voltage is reset. The resulting spike is sent to other neurons in the network. The excitable laser is composed of a gain section, SA, and mirrors for cavity feedback. The inputs selectively perturb the gain optically or electrically. The gain medium acts as a temporal integrator while the SA acts as a threshold detector; it extracts most of the stored energy from the gain medium into the optical mode. These dynamics emulate *excitability*, one of the most critical properties of a spiking neuron.

negative, and delayed by t_j resulting in a time series that is spatially summed. This aggregate input induces an electrical current, $I_{app} = V_m(t) \sum_{j=1}^{N} w_j x_j(t - t_j)$ between adjacent neurons, where the membrane potential $V_m(t)$, the voltage difference across their membrane, acts as the primary internal (activation) state variable. The weights and delays determine the dynamics of network, providing a way of programming a neuromorphic system. The soma acts as a first-order low-pass filter or a leaky integrator, with the integration time constant $t_m = R_m C_m$ that

$V_m(t)$ recovers from V_{reset} to the resting potential V_L in which is difficult to induce the firing of a spike. Consequently, the output of the neuron consists of a series of spikes that occur at continuously valued times. There are three influences on $V_m(t)$: passive leakage of current, an active pumping current, and external inputs generating time-varying membrane conductance changes. Including a set of digital conditions, we arrive at a typical LIF model for an individual neuron:

$$\underbrace{\frac{dV_m(t)}{dt}}_{\text{Activation}} = \underbrace{\frac{V_L}{\tau_m}}_{\text{Active pumping}} \quad \underbrace{\frac{V_m(t)}{\tau_m}}_{\text{Leakage}} + \underbrace{\frac{1}{C_m} I_{app}(t)}_{\text{External input}}; \tag{1a}$$

$$\text{if } V_m(t) > V_{thresh} \text{ then} \tag{1b}$$
$$\text{release a pulse and set } V_m(t) \, ! \quad V_{reset}.$$

2.2. Excitable laser model

Next, we briefly summarize the recently discovered mathematical analogy between the LIF neuron model and an excitable laser composed of a gain section with an embedded SA [7, 38] as illustrated in Fig. 1. The gain medium acts as a temporal integrator with a time constant that is equal to the carrier recombination lifetime. The SA extracts most of the stored energy from the gain medium into the optical mode and performs the function of a threshold detector. This gain-absorber interplay emulates one of the most critical dynamical properties of a spiking neuron—excitability.

The Yamada model [39], describes the behavior of lasers with independent gain and SA sections with an approximately constant intensity profile across the cavity. We assume that the dynamics operate such that the gain is a slow variable, while the intensity and loss are both fast. This three-dimensional dynamical system can be described with the following equations: (1) $\dot{G}(t) = g_G[A \quad G(t) \quad G(t)I(t)]$; (2) $\dot{Q}(t) = g_Q[B \quad Q(t) \quad aQ(t)I(t)]$; and (3)

Comparing this to the LIF model, or equation (1), the analogy between the equations becomes clear. Setting the variables g_G

3.2. Equivalent circuit

For a given set of injection currents $fI_a; I_sg$ in the gain and SA regions, operating point analysis of the excitable laser described by the rate equations (3)–(5) and output power (6) leads to four solutions. In addition to the correct nonnegative solution regime, in which the solutions for the photon density N_{ph}, and carrier densities n_a and n_s, are all nonnegative when $I_a \geq 0$ and $I_s \geq 0$, there are also negative-power and a high-power regimes. It is therefore necessary to transform the carrier population density in the respective cavities n_c and the laser output power P_{out} via the following pair of transformations, respectively [41]:

$$n_a = n_{eq;a} \exp \frac{q v_a}{nkT} \tag{7}$$

$$n_s = n_{eq;s} \exp \frac{q v_s}{nkT} \tag{8}$$

$$P_{out} = (v_m + d)^2 \tag{9}$$

where $n_{eq;c}$ is the equilibrium carrier density, v_c is the voltage across the gain and SA region of the laser, n is a diode ideality factor (typically set to two for III-V devices [44, 45]), v_m is a new
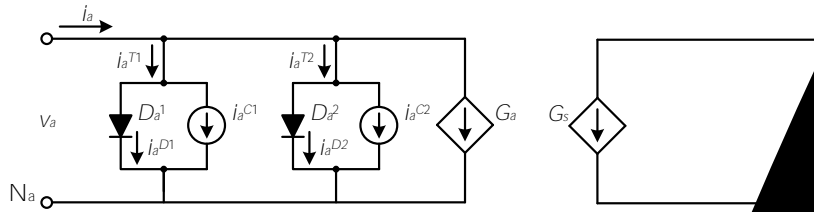
Fig. 2. Circuit-level implementation to model

These equations can be mapped directly into an equiva
Fig. 2, where $\{P_a; N_a\}$ and $\{P_s; N_s\}$ are the electrical (+
SA regions, respectively. Diodes $\{D_a^1; D_a^2\}$ and $\{D_s^1; D$
$\{i_s^{C1}; i_s^{C2}\}$, model the linear recombination and charge
respectively. The nonlinear dependent current source
emission on the carrier densities in both the gain and

Similarly, to model the photon dynamics $dN_{ph}=d$
and the output power (6), into the rate equation (5
tions, we obtain

$$2(v_m + d)\frac{dv_m}{dt} = \quad \frac{(v_m + d)^2}{t_{ph}} + \sqcap \Gamma_a g$$

With some additional rearrangements and the
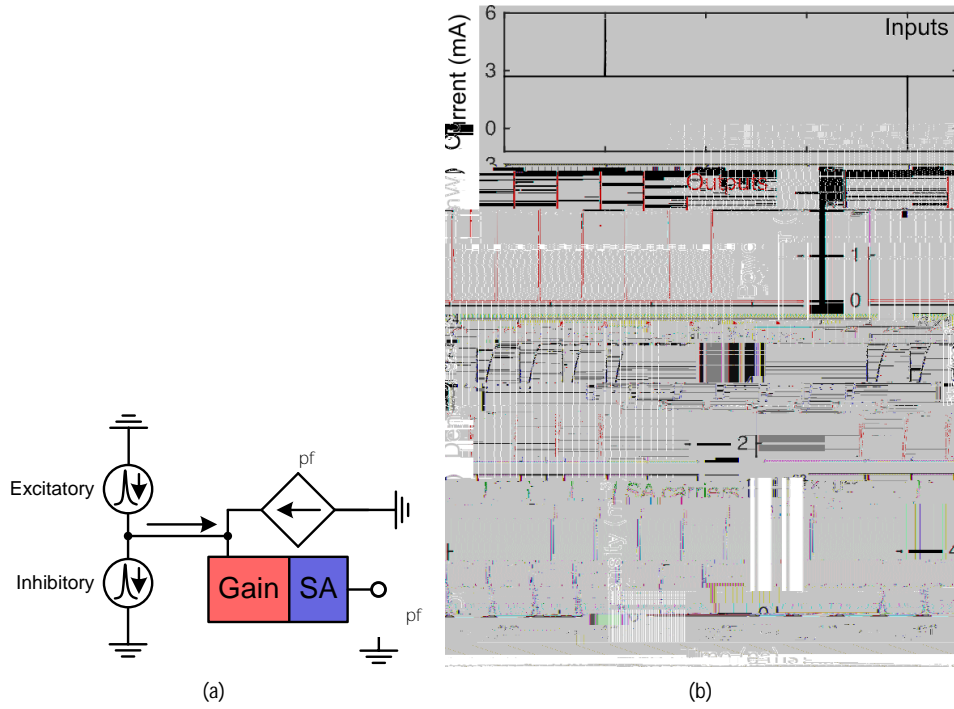be written as

$$C_{ph}m$$

Fig. 6. (a) Laser neuron circuit setup to investigating bistable dynamics. Note that the dc biasing conditions have been left out for the sake of brevity. (b) Simulation of the excitable VCSEL neuron system exhibiting bistability with connection delays of 4 ns. Top row: in-

Hodgkin–Huxley model [36]. While variable latency can lead to jitter in synchronous systems, it has also been proposed as a mechanism for converting continuous amplitude to spike-timing